Published in "Nature doi:10.1038/nature11001, 2012"
which should be cited to refer to this work.

A novel putative auxin carrier family regulates intracellular auxin homeostasis in plants

Elke Barbez[1,2], Martin Kubeš[3], Jakub Rolčík[4], Chloé Béziat[1,2], Aleš Pěnčík[5], Bangjun Wang[6], Michel Ruiz Rosquete[1,2], Jinsheng Zhu[6], Petre I. Dobrev[3], Yuree Lee[7], Eva Zažímalová[3], Jan Petrášek[3], Markus Geisler[6], Jiří Friml[1] & Jürgen Kleine-Vehn[1,2]

The phytohormone auxin acts as a prominent signal, providing, by its local accumulation or depletion in selected cells, a spatial and temporal reference for changes in the developmental program[1–7]. The distribution of auxin depends on both auxin metabolism (biosynthesis, conjugation and degradation)[8–10] and cellular auxin transport[11–15]. We identified *in silico* a novel putative auxin transport facilitator family, called PIN-LIKES (PILS). Here we illustrate that PILS proteins are required for auxin-dependent regulation of plant growth by determining the cellular sensitivity to auxin. PILS proteins regulate intracellular auxin accumulation at the endoplasmic reticulum and thus auxin availability for nuclear auxin signalling. PILS activity affects the level of endogenous auxin indole-3-acetic acid (IAA), presumably via intracellular accumulation and metabolism. Our findings reveal that the transport machinery to compartmentalize auxin within the cell is of an unexpected molecular complexity and demonstrate this compartmentalization to be functionally important for a number of developmental processes.

Prominent auxin carriers with fundamental importance during plant development are PIN-FORMED (PIN) proteins[1–3,6,9,15]. PIN1-type auxin carriers regulate the directional intercellular auxin transport at the plasma membrane. In contrast, atypical family member PIN5 regulates intracellular auxin compartmentalization into the lumen of the endoplasmic reticulum and its role in auxin homeostasis was recently identified[15,16]. PIN proteins have a predicted central hydrophilic loop, flanked at each side by five transmembrane domains. We screened *in silico* for novel PIN-like putative carrier proteins with a predicted topology similar to PIN proteins (Fig. 1a and Supplementary Fig. 2) and identified a protein family of seven members (Fig. 1b) in *Arabidopsis thaliana*, which we designated as the PILS proteins. In contrast to the similarities in the predicted protein topology, PIN and PILS proteins do not show pronounced protein sequence identity (10–18%), which limits the identification of PILS proteins by conventional, reciprocal basic local alignment search tool (BLAST) approaches. However, the distinct PIN and PILS protein families contain both the InterPro auxin carrier domain which is an *in-silico*-defined domain, aiming to predict auxin transport function (http://www.ebi.ac.uk/panda/InterPro.html). The PILS putative carrier family is conserved throughout the whole plant lineage, including unicellular algae (such as *Ostreococcus tauri* and *Chlamydomonas reinhardtii*) (Supplementary Fig. 3) where PIN proteins are absent[16], indicating that PILS proteins are evolutionarily older.

PILS genes are broadly expressed in various tissues (Fig. 1c) and *PILS2–PILS7* were transcriptionally upregulated by auxin application in wild-type seedlings (Fig. 1d–f and Supplementary Fig. 4), indicating a role in auxin-dependent processes. To investigate the potential function of the putative PILS auxin flux facilitators in plant development, we overexpressed PILS proteins using the constitutive, viral *35S* promoter. Ectopic expression of *PILS* genes, such as *PILS1* or *PILS3*, resulted in dwarfed and/or bushy plants showing severe defects in flower development, leading to sterility in the T1 generation (Fig. 2a–d). Flowers of these *PILS*-overexpressing plants showed severe patterning defects, such as homeotic transformation of flower organs into new flower buds, triplication of the gynoecium or unfused carpels (Fig. 2b–d). To circumvent sterility, we screened for weaker *p35S::PILS* lines and isolated moderately *PILS5* overexpressing lines showing fertile flower development.

To assess further the developmental importance and potential redundancy of PILS proteins in auxin-regulated processes, we focused

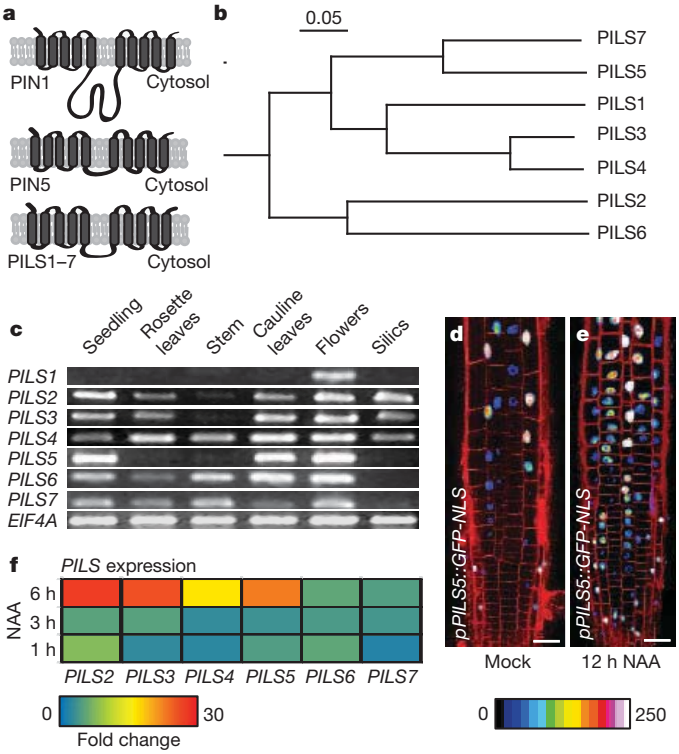

Figure 1 | Novel PILS protein family. **a**, Predicted topology of both PIN1-/PIN5-type PIN subfamilies and PILS proteins. **b**, Phylogenetic tree of the *A. thaliana* PILS proteins. Scale depicts 0.05 substitutions per position. **c**, Reverse transcription PCR (RT–PCR) of the seven *PILS* genes and *EIF4A* (control) in several plant tissues. **d**, **e**, 1-Naphthaleneacetic acid (NAA; 10 μM, 12 h)-induced *pPILS5::GFP-NLS* (GFP fused to nuclear localisation signal, NLS) expression in the root transition zone. Colour-code (black to white) depicts (low to high) GFP signal intensity. Propidium-iodide-stained cell walls in red. Scale bar, 25 μm. **f**, Quantitative RT–PCR of *PILS2–7* after 10 μM NAA treatment for 1, 3 and 6 h. Colour code from blue (low) to red (high) depicts fold changes (0–30) (see also Supplementary Fig. 4).

[1]Department of Plant Systems Biology, VIB and Department of Plant Biotechnology and Bioinformatics, Ghent University, 9052 Gent, Belgium. [2]Department of Applied Genetics and Cell Biology, University of Natural Resources and Life Siences (BOKU), 1190 Vienna, Austria. [3]Institute of Experimental Botany, The Academy of Sciences of the Czech Republic, 16502 Praha 6, Czech Republic. [4]Laboratory of Growth Regulators, Faculty of Science, Palacký University and Institute of Experimental Botany AS CR, Šlechtitelů 11, 78371 Olomouc, Czech Republic. [5]Centre of the Region Haná for Biotechnological and Agricultural Research, Department of Growth Regulators, Faculty of Science, Palacký University, Šlechtitelů 11, 78371 Olomouc, Czech Republic. [6]Department of Biology - Plant Biology, University of Fribourg, Chemin du Musée 10, 1700 Fribourg, Switzerland. [7]Department of Plant Molecular Biology, University of Lausanne, Quartier Sorge, 1015 Lausanne, Switzerland.

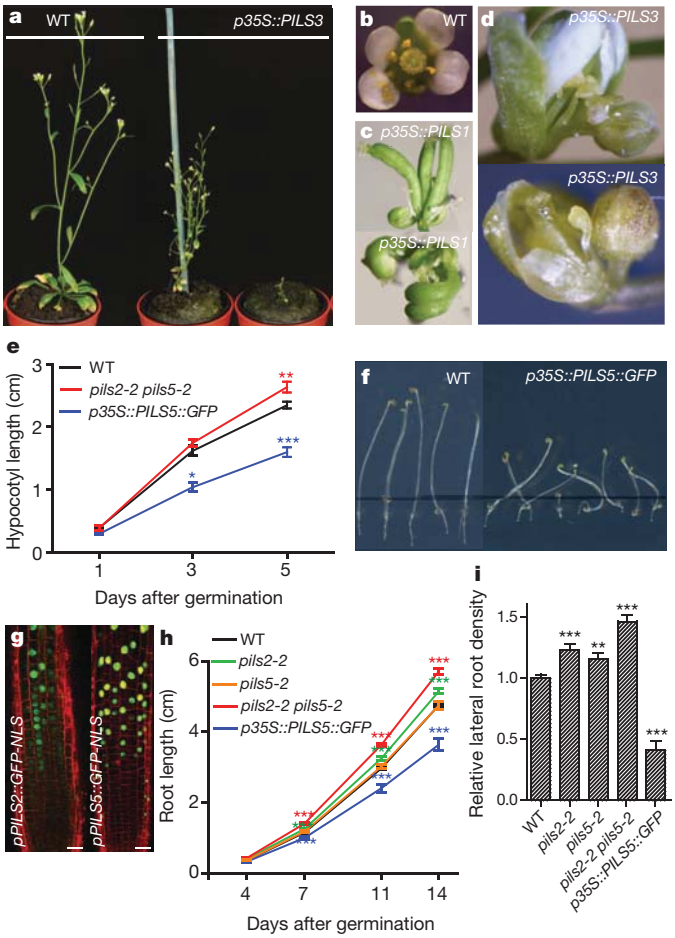

Figure 2 | Phenotypes of PILS loss- and gain-of function mutants. **a**–**d**, Wild-type (WT) and T1 transgenics strongly expressing *p35S::PILS*, such as *p35S::PILS3* (a), are sterile and show dwarfy growth. **b**–**d**, Flowers of WT (**b**), *p35S::PILS1* (**c**) and *p35S::PILS3* (**d**). **e**, Hypocotyl length of dark-grown *pils2-2 pils5-2*, *p35S::PILS5::GFP* and WT seedlings ($n > 15$). **f**, Dark-grown WT and *p35S::PILS5* seedlings (5 days after germination). **g**, *pPILS2::GFP-NLS* (left) and *pPILS5::GFP-NLS* (right) expression in the root transition zone (green). Propidium-iodide-stained cell walls in red. Scale bar, 25 µm. **h**, **i**, Root length (**h**) and lateral root density (14 days after germination) (**i**) of *pils2-2*, *pils5-2*, *pils2-2 pils5-2*, *p35S::PILS5::GFP* and WT seedlings ($n > 40$). Error bars represent s.e.m. Student *t*-test *P*-values: $*P < 0.05$, $**P < 0.001$, $***P < 0.0001$.

on *PILS2* and *PILS5*, because they are the most abundantly expressed *PILS* genes in seedlings (Fig. 1c) and display partially overlapping expression domains (Fig. 2g). Initially, we investigated PILS function in auxin-dependent hypocotyl and root growth. Dark-grown *p35S::PILS5::GFP*-expressing (coding for a PILS5–green fluorescent protein (GFP) fusion) and *pils2 pils5* double-mutant seedlings showed reduced and enhanced hypocotyl growth, respectively (Fig. 2e and Supplementary Fig. 5). *PILS5* gain-of-function also resulted in agravitropic hypocotyl growth (Fig. 2f). *PILS2* and *PILS5* showed a particular overlapping expression in the root transition zone (Fig. 2g), suggesting a redundant role in regulating root growth. Indeed, *pils2* single-mutant and more pronounced *pils2 pils5* double-mutant seedlings showed significantly longer roots compared to wild-type seedlings, whereas seedlings overexpressing *PILS5* had shorter roots (Fig. 2h). Collectively, our data indicate the requirement of defined PILS protein activity for auxin-dependent growth regulation.

Beside the root and shoot organ growth, auxin tightly controls *de novo* organ formation such as lateral root organogenesis[1]. Intriguingly, *pils2* and *pils5* single-mutants and more pronounced *pils2 pils5* double-mutants showed higher lateral root density (Fig. 2i). On the contrary, *PILS5* gain-of-function reduced lateral rooting (Fig. 2i).

These findings indicate developmental importance of PILS proteins in auxin-regulated processes, such as *de novo* organ formation and growth regulation.

Next we investigated whether auxin responses are affected in *pils* mutants using the auxin response reporter DR5 (ref. 17). *pils2-2* knockdown and *pils5-2* knockout mutants did not show altered DR5 activity in the main root tips (Supplementary Fig. 6a), but showed higher pDR5rev::GFP signal intensity in lateral roots (Fig. 3a). Moderately *p35S::PILS5::GFP*-expressing seedlings showed a visibly reduced auxin response maximum in the very root tip of main (Fig. 3b) and lateral roots (Supplementary Fig. 6b). To distinguish between direct and indirect effects, we investigated the effect of PILS proteins on nuclear auxin signalling at the cellular level. Therefore, we transiently co-expressed *PILS2* or *PILS5* together with the auxin response reporter *pDR5rev::mRFPer* (expressing the red fluorescent protein (RFP) in response to auxin signalling) in tobacco Bright Yellow 2 (BY-2) cells. *PILS2* or *PILS5* expression in BY-2 cells reduced auxin signalling as visualized by *pDR5rev::mRFPer* activity (Fig. 3c, d). These findings indicate that PILS proteins negatively affect nuclear auxin signalling, presumably by affecting cellular auxin homeostasis.

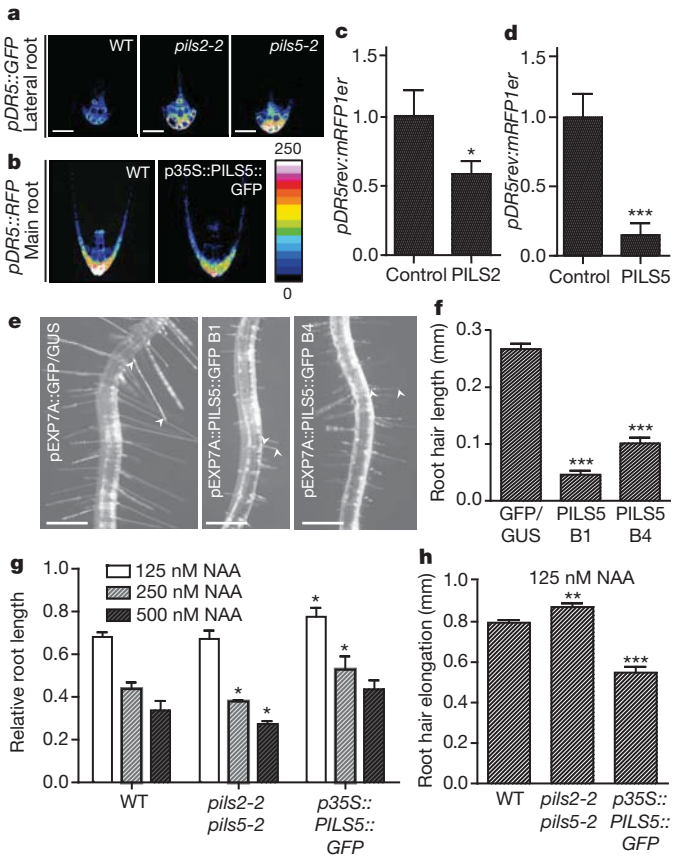

Figure 3 | PILS proteins affect auxin-dependent cellular growth. **a**, **b**, DR5 promoter activity in *pils2-2* and *pils5-2* (lateral roots) (**a**) and *p35S::PILS5::GFP* (main root) (**b**) compared to wild type (WT) (see also Supplementary Fig. 6). Colour-code (black to white) depicts (low to high) *pDR5rev::GFP* and *pDR5rev::mRFP1er* signal intensity. Scale bars, 25 µm. **c**, **d**, Mean grey value of *pDR5rev::mRFP1er* signal intensity in BY-2 cells expressing *p35S::PILS2* (**c**) or *p35S::PILS5* (**d**) compared to control cells (*p35S::GFP::HDEL*) ($n > 60$ cells). **e**, **f**, Root hair length (**e**, arrowheads) and quantification (**f**) of transgenic lines expressing *pEXP7A::GFP::GUS* (control) and *pEXP7A::PILS5:GFP* (independent lines B1 and B4) ($n = 20$ seedlings with 400 counted root hairs in total). Scale bars, 250 µm. **g**, Relative root length of NAA-treated *pils2-2 pils5-2* and *p35S::PILS5::GFP* seedlings compared to WT ($n > 20$). **h**, Auxin-induced root hair elongation ($n = 20$ seedlings with 400 counted root hairs in total). Mean untreated root hair length was subtracted from the treated values. Error bars represent s.e.m. Student *t*-test P-values: $*P < 0.05$, $**P < 0.001$, $***P < 0.0001$.

To address whether cellular PILS action on auxin signalling affects cellular growth, we expressed *PILS1*, *PILS3* and *PILS5* under a root-hair-specific promoter. Deviations in free (active) indole-3-acetic acid (IAA) levels or in auxin signalling induce (high levels) or repress (low levels) root hair growth[18]. As expected, the root-hair-specific expression of *PILS1*, *PILS3* and *PILS5* significantly reduced root hair length (Fig. 3e, f and Supplementary Fig. 7a–c), possibly due to PILS-dependent regulation of auxin homeostasis and signalling.

Next we tested whether PILS proteins affect auxin-dependent cellular growth responses. We treated PILS gain- and loss-of-function mutants with auxin that inhibits primary root growth. *pils2 pils5* loss- and *PILS5* gain-of-function mutants showed hyper- and hyposensitive root growth, respectively (Fig. 3g). In agreement with these observations, the auxin-promoted root hair growth was also enhanced in *pils2 pils5* double-mutants and reduced in *PILS5* overexpressers (Fig. 3h). This set of data indicates that PILS putative auxin facilitators modulate auxin-dependent growth responses during plant development.

To unravel the mechanism by which PILS proteins regulate auxin-dependent plant development, we investigated the subcellular localization of PILS proteins. We introduced amino- or carboxy-terminal GREEN/RED FLUORESCENT PROTEIN (GFP/RFP) fusions with PILS proteins and transiently or stably expressed these fusion proteins in tobacco BY-2 cell culture, *Arabidopsis* seedlings and heterologously in yeast (Fig. 4a–c and Supplementary Fig. 8). PILS1, PILS2, PILS3, PILS5, PILS6 and PILS7 GFP/RFP fusion proteins localized to the endoplasmic reticulum in all analysed systems (Fig. 4a–c and Supplementary Figs 8 and 10c). In contrast, N- and C-terminal PILS4 fusions did not show detectable fluorescence. The transgenic *pPILS5::PILS5::GFP* also showed endoplasmic reticulum localization (Fig. 4a) and complemented the *pils2 pils5* double-mutant to the *pils2* single-mutant level (Supplementary Fig. 9), indicating PILS function at the endoplasmic reticulum.

Next, we addressed whether putative PILS auxin carriers affect cellular auxin accumulation. We generated *PILS2* oestradiol-inducible tobacco BY-2 cell cultures and performed ^{3}H-IAA accumulation assays. *PILS2* induction increased the accumulation of radioactivity in BY-2 cells (Fig. 4d). In accordance with the auxin accumulation assays in BY-2 cells, *pils2 pils5* double-mutant protoplasts showed significantly higher auxin export (Fig. 4e and Supplementary Fig. 10a), indicating reduced auxin retention capacity in *pils2 pils5* loss-of-function mutants. These gain and loss-of-function studies consistently illustrate that PILS2 and PILS5 function at the endoplasmic reticulum controls cellular accumulation of auxin.

To additionally address PILS protein function in a non-plant system, we expressed *PILS3*, *PILS5* and *PILS7* (tagged to GFP or haemagglutinin (HA)) in *Saccharomyces cerevisiae* yeast cells. In accordance with the effect of PILS2 and PILS5 in plant cells, the expression of *A. thaliana PILS3*, *PILS5* and *PILS7* in yeast also increased retention of exogenously applied auxin (Fig. 4f and Supplementary Fig. 10b). To assess the specificity to auxin we used the common organic control benzoic acid (BA). Notably, PILS3, PILS5 and PILS7 did not affect the cellular accumulation of BA (Fig. 4f and Supplementary Fig. 10b). These findings indicate that PILS proteins specifically regulate cellular auxin accumulation.

PILS proteins increase cellular auxin accumulation, but decrease auxin signalling, which is reminiscent of the regulation of auxin metabolism shown for the PIN5 auxin transporter[16]. To assess the potential action of PILS proteins on auxin metabolism, we analysed the effect of PILS proteins on the auxin metabolism using the inducible *PILS2* BY-2 cell line. The high-performance liquid chromatography (HPLC) chromatogram of IAA showed a PILS2-dependent reduction of free IAA within 20 min (Fig. 4g, h), indicating that PILS2 activity affects auxin metabolism.

In accordance with the auxin metabolite profiling in BY-2 cell cultures, *pils2*, *pils5* and *pils2 pils5* mutant *Arabidopsis* seedlings showed significantly higher free IAA levels compared to wild-type seedlings (Fig. 4i). Intriguingly, the ratio of amid auxin conjugates IAA-Glutamate (Glu) and IAA-Aspartate (Asp) to free IAA was also significantly shifted towards free IAA in *pils2* and *pils5* loss-of-function mutants (Fig. 4j, k). Moderately *p35S::PILS5::GFP*-expressing seedlings showed a visibly reduced auxin response maximum in the very root tip (Fig. 3b), but only a mild and statistically non significant reduction in free IAA levels

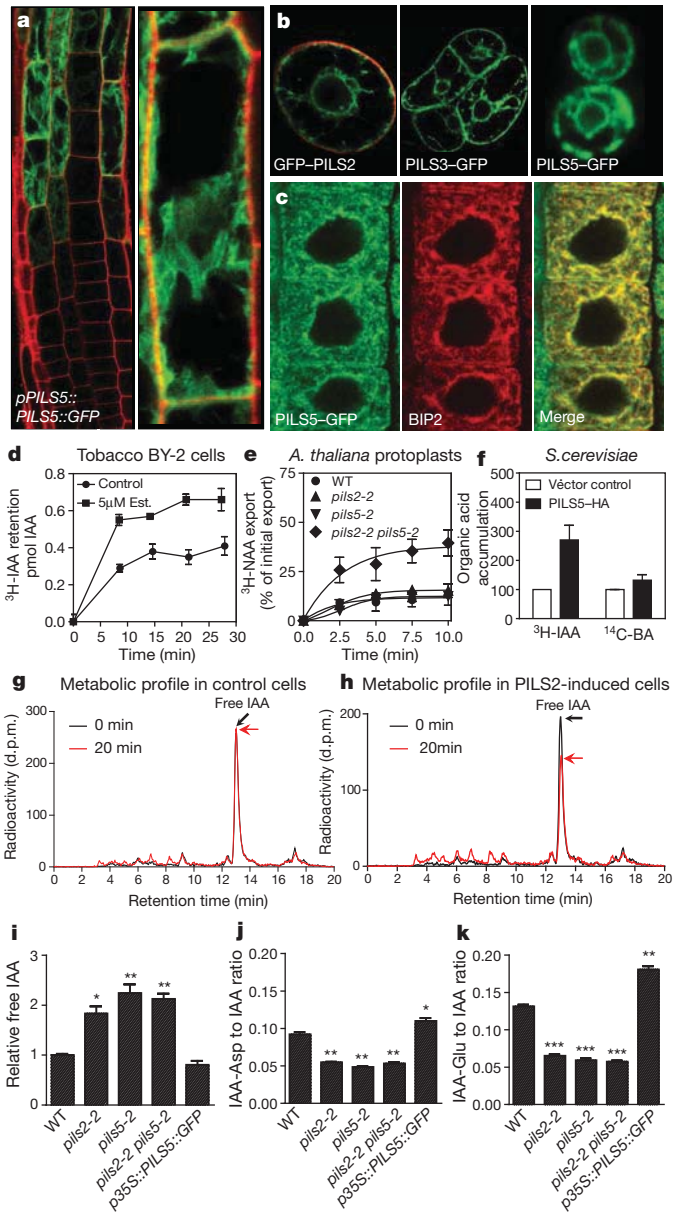

Figure 4 | PILS involvement in cellular auxin homeostasis. **a**–**c**, GFP–PILS2 (**b**), PILS3–GFP (**b**), PILS5–GFP (**a**–**c**) under endogenous (**a**) or constitutive promoter (**b**, **c**) in *A. thaliana* root (**a**, **c**), tobacco BY-2 cells (**b**, left panels) and *Saccharomyces cerevisiae* yeast cells (**b**, right panel). **c**, Immunocytochemistry of PILS5–GFP and the endoplasmic reticulum marker BIP2. **d**, ^{3}H-IAA retention in tobacco BY-2 cells upon oestradiol (Est.)-induced *PILS2* expression ($n = 3$ repetitions). **e**, ^{3}H-NAA export assay in *A. thaliana* protoplasts of wild type (WT), *pils2-2*, *pils5-2* and *pils2 pils5* mutants ($n = 3$ repetitions; see also Supplementary Fig. 10a). **f**, Accumulation of auxin and benzoic acid in *Saccharomyces cerevisiae* yeast cells transformed with *pGPD::PILS5::HA* or an empty vector ($n = 3$ repetitions; see also Supplementary Fig. 10b). **g**, **h**, ^{3}H-IAA metabolic profile (HPLC chromatogram) in PILS2 non-oestradiol-induced (**g**) and oestradiol-induced (**h**) tobacco BY-2 cells after 0 (black line) and 20 min (red line). **i**–**k**, Liquid chromatography-mass spectrometry (LC-MS)-derived free IAA levels (**i**) and ratios of IAA-Asp (**j**) and IAA-Glu (**k**) to free IAA in WT, *pils2-2*, *pils5-2*, *pils2-2 pils5-2* and *p35S::PILS5::GFP* ($n = 3$ repetitions). Error bars represent s.e.m. Student *t*-test P-values: $^{*}P < 0.05$, $^{**}P < 0.001$, $^{***}P < 0.0001$. Scale bar, 10 μm.

at the whole seedling level (Fig. 4i). However, the ratio of IAA-Glu and IAA-Asp to free IAA was significantly shifted towards the conjugates in *p35S::PILS5::GFP* seedlings (Fig. 4j, k), indicating a higher rate of auxin conjugation.

These findings are indicative of a PILS function in cellular auxin homeostasis by regulating auxin metabolism. Hence, we propose a model in which PILS proteins at the endoplasmic reticulum membrane facilitate intracellular auxin accumulation, which seems to contribute to the possibly compartmentalized regulation of auxin metabolism (Supplementary Fig. 1). It is tempting to speculate that auxin conjugation could also take place in the endoplasmic reticulum, although the molecular components remain to be identified.

Our *in silico* and reverse genetics approaches led to the identification of a novel family of putative auxin transport facilitators. All our genetic, pharmacological, cell biological, physiological and biochemical approaches consistently suggest that PILS proteins function at the endoplasmic reticulum membrane, regulate intracellular auxin accumulation and affect free IAA levels, presumably through conjugation-based auxin metabolism. The PILS action on cellular auxin homeostasis is reminiscent of the function of the atypical PIN family member PIN5 (ref. 16). We uncovered that an additional, distinct protein family regulates intracellular auxin homeostasis. Our analyses of the PILS proteins suggest that intracellular auxin transport and, hence, auxin compartmentalization might be evolutionarily older than directional, cell-to-cell PIN-dependent auxin transport mechanisms. The identification of a novel protein family for the regulation of intracellular auxin homeostasis highlights the evolutionary and developmental importance of intracellular auxin transport. Further studies will address the potential interplay or possible diversified function of endoplasmic reticulum localized PIN5 and PILS1–7 proteins.

METHODS SUMMARY

Plant material and growth conditions. We used *Arabidopsis thaliana* of ecotype Columbia 0 (Col-0). The *Nicotiana tabacum* L. cv. Bright Yellow 2 (BY-2) cell line[19] was used as suspension-cultured cells. *pils2-1* (*SALK_024808*), *pils2-2* (*SALK_125391*), *pils5-1* (*SALK_070653*) and *pils5-2* (*SALK_072996*) were obtained from the Nottingham *Arabidopsis* Stock Centre (NASC). Gateway cloning was used to construct *pPILS2::GFP/GUS*, *pPILS5::GFP/GUS*, *p35S::PILS1–7*, *p35S::GFP::PILS1–7*, *p35S::PILS1–7::GFP*, *pPILS5::PILS5::GFP* and *pMDC7_B(pUBQ)::PILS2*. The following lines and constructs have been previously described: *pDR5rev::mRFP1er*[20], *pDR5rev::GFP*[2] and *p35S::GFP::HDEL*[21]. Seeds were stratified at 4 °C for 2 days in the dark. Seedlings were grown vertically on half Murashige and Skoog medium. Plants were grown under long-day (16 h light/8 h dark) conditions at 20–22 °C.

1. Benková, E. *et al.* Local, efflux-dependent auxin gradients as a common module for plant organ formation. *Cell* **115,** 591–602 (2003).
2. Friml, J. *et al.* Efflux-dependent auxin gradients establish the apical-basal axis of *Arabidopsis*. *Nature* **426,** 147–153 (2003).
3. Reinhardt, D. *et al.* Regulation of phyllotaxis by polar auxin transport. *Nature* **426,** 255–260 (2003).
4. Leyser, O. Dynamic integration of auxin transport and signalling. *Curr. Biol.* **16,** R424–R433 (2006).
5. Dubrovsky, J. G. *et al.* Auxin acts as a local morphogenetic trigger to specify lateral root founder cells. *Proc. Natl Acad. Sci. USA* **105,** 8790–8794 (2008).
6. Sorefan, K. *et al.* A regulated auxin minimum is required for seed dispersal in *Arabidopsis*. *Nature* **459,** 583–586 (2009).
7. Prasad, K. *et al. Arabidopsis* PLETHORA transcription factors control phyllotaxis. *Curr. Biol.* **21,** 1123–1128 (2011).
8. Woodward, A. W. & Bartel, B. Auxin: regulation, action, and interaction. *Ann. Bot.* **95,** 707–735 (2005).
9. Ikeda, Y. *et al.* Local auxin biosynthesis modulates gradient-directed planar polarity in *Arabidopsis*. *Nature Cell Biol.* **11,** 731–738 (2009).
10. Zhao, Y. Auxin biosynthesis and its role in plant development. *Annu. Rev. Plant Biol.* **61,** 49–64 (2010).
11. Bennett, M. J. *et al. Arabidopsis AUX1* gene: a permease-like regulator of root gravitropism. *Science* **273,** 948–950 (1996).
12. Luschnig, C., Gaxiola, R. A., Grisafi, P. & Fink, G. R. EIR1, a root-specific protein involved in auxin transport, is required for gravitropism in *Arabidopsis thaliana*. *Genes Dev.* **12,** 2175–2187 (1998).
13. Geisler, M. *et al.* Cellular efflux of auxin catalyzed by the *Arabidopsis* MDR/PGP transporter AtPGP1. *Plant J.* **44,** 179–194 (2005).
14. Petrášek, J. *et al.* PIN proteins perform a rate-limiting function in cellular auxin efflux. *Science* **312,** 914–918 (2006).
15. Zažímalová, E., Murphy, A. S., Yang, H., Hoyerová, K. & Hošek, P. Auxin transporters–why so many? *Cold Spring Harb. Perspect. Biol.* **2,** a001552 (2010).
16. Mravec, J. *et al.* ER-localized PIN5 auxin transporter mediates subcellular homeostasis of phytohormone auxin. *Nature* **459,** 1136–1140 (2009).
17. Ulmasov, T., Murfett, J., Hagen, G. & Guilfoyle, T. J. Aux/IAA proteins repress expression of reporter genes containing natural and highly active synthetic auxin response elements. *Plant Cell* **9,** 1963–1971 (1997).
18. Lee, S. H. & Cho, H. T. PINOID positively regulates auxin efflux in *Arabidopsis* root hair cells and tobacco cells. *Plant Cell* **18,** 1604–1616 (2006).
19. Nagata, T., Nemoto, Y. & Hasezawa, S. Tobacco BY-2 cell line as the "HeLa" cells in the cell biology of higher plants. *Int. Rev. Cytol.* **132,** 1–30 (1992).
20. Marin, E. *et al.* miR390, *Arabidopsis TAS3* tasiRNAs, and their *AUXIN RESPONSE FACTOR* targets define an autoregulatory network quantitatively regulating lateral root growth. *Plant Cell* **22,** 1104–1117 (2010).
21. Langhans, M. *et al. In vivo* trafficking and localization of p24 proteins in plant cells. *Traffic* **9,** 770–785 (2008).

Acknowledgements We are grateful to C. Braeckman for plant transformation; W. Ardiles for sequencing support; L. Charrier for technical assistance; A. Maizel, N. Geldner and P. Pimpl for providing material; J.K.-V. group members for critical reading of the manuscript and the BOKU-VIBT Imaging Center for access and expertise. This work was supported by the Vienna Science and Technology Fund (WWTF) (to J.K.-V.), the Agency for Innovation by Science and Technology (IWT) (predoctoral fellowship to E.B.), the Odysseus program of the Research Foundation-Flanders (to J.F.), the Swiss National Funds (to M.G.), the Ministry of Education, Youth and Sports of the Czech Republic (LC06034) (to E.Z.), Grant Agency of the Czech Republic project P305/11/2476 (to J.P.) and P305/11/0797 (to E.Z).

Author Contributions E.B. and J.K.V. conceived the project. E.B. carried out most of the experiments. M.K., P.I.B., E.Z. and J.P. performed auxin metabolite profile and auxin accumulation in BY-2. C.B. analysed auxin-dependent PILS expression and contributed to phenotype analysis. M.R.R. contributed to PILS cloning. J.R. and A.P. measured auxin content in *Arabidopsis*. B.W., J.Z. and M.G. performed auxin accumulation in yeast and protoplasts. Y.L. modified the oestradiol-inducible vector. E.B., M.K., J.R., E.Z., J.P., M.G., J.F. and J.K.V. discussed the experimental procedures. All authors analysed and discussed the data; E.B. and J.K.V. wrote the paper and all authors saw and commented on the manuscript.

METHODS

***PILS* gene accession codes.** Sequence data from this article can be found in The *Arabidopsis* Information Resource (TAIR; http://www.arabidopsis.org/) or GenBank/EMBL databases under the following accession numbers: *PILS1* (At1g20925), *PILS2* (At1g71090), *PILS3* (At1g76520), *PILS4* (At1g76530), *PILS5* (At2g17500), *PILS6* (At5g01990), *PILS7* (At5g65980).

Plant material, growth conditions and DNA constructs. We used *Arabidopsis thaliana* of ecotype Columbia 0 (Col-0). The *Nicotiana tabacum* L. cv. Bright Yellow 2 (BY-2) cell line[19] was used as suspension-cultured cells. *pils2-1* (*SALK_024808*), *pils2-2* (*SALK_125391*), *pils5-1* (*SALK_070653*) and *pils5-2* (*SALK_072996*) were obtained from the Nottingham *Arabidopsis* Stock Centre (NASC). Insertion sites were verified, homozygous lines selected and the decrease or absence of the respective *PILS* transcript was shown by RT–PCR. The *pils2-2* and the *pils5-2* mutants were crossed into *DR5rev::GFP*[2]. Gateway cloning was used to construct *pPILS2::GFP::GUS*, *pPILS5::GFP::GUS*, *p35S::PILS1–7*, *p35S::GFP::PILS1–7*, *p35S::PILS1–7::GFP*, *pPILS5::PILS5::GFP* and *pMDC7_B(pUBQ)::PILS2*. The *PILS* full-length genomic fragments, complementary DNA and promoter regions were amplified by PCR from genomic DNA and cDNA, respectively. The PCR was performed using the high fidelity DNA polymerase "I proof" (Bio-Rad). The primers used are given below. The full genomic and cDNA fragments were cloned into the pDONR221 (Invitrogen) vector and the promoter regions into pDONR-P4P1 using Invitrogen BP-clonase according to manufacturer's instructions. Coding sequences were transferred from the entry clones to gateway-compatible destination vectors (given below) using the Invitrogen LR clonase(+) according to manufacturer's instructions. The resulting constructs were transformed into Col-0 plants by floral dipping in *Agrobacterium tumefaciens* liquid cultures. Yeast vectors were transformed into budding yeast (*Saccharomyces cerevisiae*) via electroporation. The *p35S::PILS5::GFP* line was crossed into *pDR5rev::mRFP1er*[20]. The following lines and constructs have been previously described: *pDR5rev::mRFP1er*[20], *pDR5rev::GFP*[2] and *p35S::GFP::HDEL*[21]. Seeds were stratified at 4 °C for 2 days in the dark. Seedlings were grown vertically on half Murashige and Skoog medium. Plants were grown under long-day (16 h light/8 h dark) conditions at 20–22 °C.

Chemicals. 1-Naphthaleneacetic acid (NAA) was supplied by Duchefa, 2,4-dichlorophenoxy acetic acid, oestradiol and propidium iodide by Sigma-Aldrich and ^{3}H-indole-3-acetic acid (^{3}H-IAA), ^{3}H-naphthalene-1-acetic acid (^{3}H-NAA) and ^{14}C-benzoic acid (^{14}C-BA) (specific radioactivity 20 Ci mmol^{-1}) by American Radiolabelled Chemicals.

RNA extraction and quantitative real time PCR (qPCR). Whole RNA of seedlings was extracted using the RNeasy Mini Kit (Qiagen) in technical triplicates, the extracted RNA samples were treated with DNase (Ambion). qPCR analysis was performed using ICycler (Bio-Rad) with the Platinum SYBR Green qPCR Super-UDG kit (Invitrogen) following recommendations of the manufacturer. qPCR was carried out in 96-well optical reaction plates heated for 10 min to 95 °C to activate hot-start *Taq* DNA polymerase, followed by 40 cycles of denaturation for 60 s at 95 °C and annealing-extension for 60 s at 58 °C. Target quantifications were performed with specific primer pairs (given later) designed using Beacon Designer 4.0 (Premier Biosoft International). Expression levels were normalized to the expression levels of translation initiation factor EIF4A. The primers used are given later.

Phenotype analysis. For analysis of the root length and lateral root density, plates were scanned on a flat-bed scanner. Root hairs were imaged with a binocular microscope (Leica). For hypocotyls analysis, seeds on plates were exposed to light for 3 h at 18 °C, and cultivated in the dark at 20 °C. Seedlings were imaged in real time with an infrared camera (Canon) to define the exact moment of germination and analysed 1, 3 and 5 days after germination. Hypocotyls, root and root hair lengths were measured with the ImageJ (http://rsb.info.nih.gov/ij/) software. Lateral root density for each seedling was obtained by calculating the number of lateral roots per root length unit 14 days after germination. For analysis of hypocotyls length, a minimum of 15 hypocotyls per condition or mutant line were analysed in each experiment. For analysis of root length and lateral root density, a minimum of 40 plants per condition or mutant line were analysed in each experiment. Means and standard errors were calculated and the statistical significance was evaluated by the student *t*-test using the GraphPad Prism5 (http://www.graphpad.com) software. For the analysis of root hair growth, 20 seedlings per transgenic line were imaged by binocular (Leica) and 20 root hairs (randomly chosen in the root hair zone) per seedling were measured with the ImageJ (http://rsb.info.nih.gov/ij/) software. The mean and standard error of the mean per transgenic line were calculated and the statistical significance was evaluated by the student *t*-test. To obtain the auxin-dependent root hair elongation, the same number of root hairs per seedling, seedlings per mutant line and condition were analysed as described above. The untreated mean average root hair length of the respective genotype was subtracted from the individual auxin-treated root hair length to obtain auxin induced growth in millimetre. The mean and standard error of the mean of the respective genotype were calculated and the statistical significance was evaluated by the student *t*-test using the GraphPad Prism5 (http://www.graphpad.com) software. All experiments were performed in at least three independent biological repetitions.

BY-2 plant material. Cells of tobacco line BY-2 (*Nicotiana tabacum* L., cv. Bright Yellow 2)[19] transformed with *pMDC7_B(pUBQ)::PILS2* were cultured in liquid cultivation medium (3% (w/v) sucrose, 4.3 g l^{-1} Murashige and Skoog salts, 100 mg l^{-1} inositol, 1 mg l^{-1} thiamine, 0.2 mg l^{-1} 2,4-dichlorophenoxy acetic acid, and 200 mg l^{-1} KH_2PO_4 (pH 5.8). BY-2 cell lines were cultivated in darkness at 26 °C on an orbital incubator (Sanyo Gallenkamp, Schöeller Instruments; 150 r.p.m., 32-mm orbit) and subcultured weekly. Stock BY-2 calli were maintained on media solidified with 0.6% (w/v) agar and subcultured monthly.

Transient transformation of BY-2 cells and monitoring of cellular auxin signalling in BY2. Ten ml of three-day-old cells were harvested on filter paper by vacuum filtration and kept on plates with solid BY-2 medium. The cells were transformed via particle bombardment with a PDS 1000/He biolistic system (Bio-Rad) according to the manufacturer's instructions (http://www.bio-rad.com/webroot/web/pdf/lsr/literature/Bulletin_9075.pdf). 2 µl of plasmid DNA (0.05 µg µl of the *pDR5rev::mRFP1er* contruct and 0.1 µg µl^{-1} of *p35S::PILS2* and *p35S::PILS5*) was added to 6.25 µl of 1.6-µm diameter gold particles (dissolved in 50% glycerol). The suspension was supplemented with 2.5 µl spermidine (0.1 M stock solution) and 6.25 µl $CaCl_2$ (2.5 M stock solution). The particles were pelleted by centrifugation, washed twice with 70% and 100% ethanol and, subsequently, resuspended in 10 µl of 100% ethanol. Cells were bombarded under a pressure of 1,100 pounds per square inch. The plates were sealed with Parafilm and kept in the dark for 18 h at 25 °C. For microscopic analysis, cells were gently transferred from the filter to a microscopy slide (in water) and subsequently covered with a cover slip. Samples were analysed via confocal microscopy. The *pDR5rev::mRFP1er* expression was evaluated by defining the mean grey value (MGV) of each imaged cell (middle sections). For each experiment, confocal settings were defined based on the *pDR5rev::mRFP1er* signal of the control cells and remained unchanged during the respective experiments. Transformants were identified on the basis of the fluorescence of both proteins and imaged with a ×40 objective. Every experiment/transformation was done in triplicate and for each condition a total number of at least 60 transformed cells were imaged. For each experiment, the means and standard errors were calculated and the statistical significance (independence between the two populations) was obtained by the student *t*-test using the GraphPad Prism5 (http://www.graphpad.com) software.

Immunocytochemistry. Whole-mount immunological staining on 5-day-old seedlings was done in an Intavis robot according to the described protocol[22]. The antibodies used at the final dilutions were monoclonal mouse anti-BIP2 (Hsc70) at 1:200 (Stressgen Bioreagents), monoclonal rabbit anti-GFP at 1:600 (Invitrogen). The secondary anti-mouse (Invitrogen) and anti-rabbit (Sigma-Aldrich) antibodies conjugated with Cy3 and Alexa488 respectively were used at 1:600 dilution.

Microscopy. Confocal microscopy was done with a Zeiss 710 microscope (Zeiss) or Leica SP5 (Leica). Fluorescence signals for GFP (excitation 488 nm, emission peak 509 nm), mRFP1 (excitation 561 nm, emission peak 607 nm) and propidium iodide (PI) staining (excitation 536 nm, emission peak 617 nm) were detected with a ×20, ×40 (water immersion) or ×63 (water immersion) objective. Sequential scanning was used for double labelling to avoid crosstalk between channels. Fluorescence signal intensity was analysed with ImageJ (http://rsb.info.nih.gov/ij/) software and data were statistically evaluated with Microsoft Excel 2007.

Auxin transport assays in tobacco BY-2 cells, baker's yeast and *Arabidopsis thaliana* protoplasts. Auxin accumulation with 2-day-old BY-2 cells was measured as previously described[14,23]. The ^{3}H-IAA was added to give a final concentration of 2 nM. Accumulation results were expressed as pmols of particular auxin accumulated per 10^{6} cells. The 0.5-ml aliquots of cell suspension were collected continuously and accumulation of label was terminated by rapid filtration under reduced pressure on 22-mm-diameter cellulose filters. The cell cakes and filters were transferred to scintillation vials, extracted in 0.5 ml of 96% ethanol for 30 min, and afterwards 4 ml of scintillation solution (EcoLite Liquid Scintilation Fluid, MP Biomedicals) was added. Radioactivity was determined by liquid scintillation counter Packard Tri-Carb 2900TR (Packard-Canberra, Meridian). Yeast ^{3}H-IAA loading was quantified with the unspecific ^{14}C-benzoic acid as control assayed in parallel and performed as previously described[24]. Relative export is calculated from yeast-retained radioactivity as follows: ((radioactivity in the yeast at time $t = 10$ min) − (radioactivity in the yeast at time $t = 0$)) × (100%)/(radioactivity in the yeast at $t = 0$ min). Unspecific loading due to diffusion was eliminated by vector control subtraction. IAA export from *Arabidopsis thaliana* mesophyll protoplasts was analysed as described[16].

HPLC metabolic profiling in tobacco BY-2 cells. Two-days-old BY-2 cells were prepared for the experiment by equilibration in uptake buffer as already described for accumulation assays[14]. Experiments were done in uptake buffer and under

standard cultivation conditions. Cells were incubated with addition of 20 nM ^{3}H-IAA for a period of 0 and 20 min. Cells and media (uptake buffer) were collected and frozen in liquid nitrogen (100 mg of fresh weight and 5 ml per sample). Extraction and purification of auxin metabolites in cells and media were performed as described[25,26]. The metabolites were separated on HPLC consisting of autosampler and 235C diode array detector (Perkin Elmer), column Luna C18 (2), 150 × 4.6 mm, 3 µm (Phenomenex, Torrance, USA), mobile phase A: 40 mM CH_3COONH_4, (pH 4.0) and mobile phase B: CH_3CN/CH_3OH, 1/1, (v/v). Flow rate was 0.6 ml min^{-1} with linear gradient 30–50% B for 10 min, 50–100% B for 1 min, 100% B for 2 min, 10–30% B for 1 min. The column eluate was monitored on 235C DAD followed by Ramona 2000 flow-through radioactivity detector (Raytest GmbH) after online mixing with three volumes (1.8 ml min^{-1}) of liquid scintillation cocktail (Flo-Scint III, Perkin Elmer). The radioactive metabolites were identified on the basis of comparison of their retention times with authentic standards. For the results presentation the total integrated area of chromatogram plots has been normalized based on the equalization of total accumulated radiolabel.

***In silico* and phylogenetic analysis.** *PILS* genes were identified via the SMART-protein tool from EMBL (http://smart.embl-heidelberg.de/)[27,28]. Phylogenetic tree of AtPILS was constructed with the DNA-man software version 4.0. PILS topologies were defined by the online HMM-top tool (http://www.enzim.hu/hmmtop/)[29] and visualized by the TMRPres2D software (http://biophysics.biol.uoa.gr/TMRPres2D/download.jsp)[30]. PILS orthologues were identified with the online tool Plaza (http://bioinformatics.psb.ugent.be/plaza/)[31].

Free IAA and conjugate measurements in *Arabidopsis thaliana*. For the quantification of free IAA and its amino acid conjugates, approximately 10 mg of plant material was taken into analysis. The samples were processed as previously described[32] and quantified by UHPLC-MS/MS.

Used primers and vectors. Genotyping primers: pils2-1 RP, CTGGAGAAACC TGACATCTCG; pils2-1 LP, GATTGAAGCCGGCTTAAATTC; pils2-2 RP, CTGGAGAAACCTGACATCTCG; pils2-2 LP, TACCATTGATCTGTCTTCG GG; pils5-1 RP, TTGAGACCCGTATCATTGGAG; pils5-1 LP, TGTCCTG ATAAAACCTTTTCAGG; pils5-2 RP, TACTGCACCGAAAATGAAACC; pils5-2 LP, TTGTACTATTTGCACCGGCTC.

Insert primer (LBb) (combine with RP): GCGTGGACCGCTTGCTGCAACT.

RT–PCR primers used for insertion lines: PILS2 Fw, GCGATCATTATCGGATC AGT; PILS2 Rev, TTGCATACCTTGGACAGTAGTC; PILS5 Fw, TGTTGA AGCCCGTAATTCCATGAAC; PILS5 Rev, TTCATTGCGGACCCTTTAAT CAGC.

qPCR primers: PILS1 Fw, CGGTAACACAGCTCCACTTC; PILS1 Rev, GCAACAAGTAACGCACAACC; PILS2 Fw, GTGATGCTTGTACTTGGTGG TATG; PILS2 Rev, AACTTGAACATTGGATCTGCTGAG; PILS3 Fw, AGGCG ACCATGCAAGTGTTG; PILS3 Rev, GTGGTACAGCTAGATGACAGTGAG; PILS4 Fw, TGTCATAACTAAGCCTCCTTCAC; PILS4 Rev, CTCGCAACTCTC AGAATCTCC; PILS5 Fw, CTTGGAATAGTCTGTGTTCGGTAC; PILS5 Rev, GCACTGAGCATTCGTCTTGAG; PILS6 Fw, GCCTACATCAGTGCTCTCAG; PILS6 Rev, GCACTGAGCATTCGTCTTGAG; PILS7 Fw, TCCTCCAGACCCTC TCTTTCG; PILS7 Rev, ACAAGAAGATGACCGAGCACTC; EiF4a Fw, CTGGAGGTTTTGAGGCTGGTAT; EiF4a Rev, CCAAGGGTGAAAGCAAG AAGA.

Cloning primers: gDNA/cDNA: PILS1_Fw, GGGGACAAGTTTGTACAAAA AAGCAGGCTCGATGAGGATGAGGCTTTTGGATC; PILS1_Rev, GGGGAC CACTTTGTACAAGAAAGCTGGGTC(TCA)GGCTACGAGCCACATGAAG AATG; PILS2_Fw, GGGGACAAGTTTGTACAAAAAAGCAGGCTCGATGT CAGGTTTCTCCAGTGGAA; PILS2_Rev, GGGGACCACTTTGTACAAGAAA GCTGGGTC(TCA)TTGCATACCTTGGACAGTAGTCTC; PILS3_Fw, GGGG ACAAGTTTGTACAAAAAAGCAGGCTCGATGGTGAAGCTTTTGGAGCTG TTC; PILS3_Rev, GGGGACCACTTTGTACAAGAAAGCTGGGTC(TCA)AGC TACAAGCCACATGAAGAATG; PILS4_Fw, GGGGACAAGTTTGTACAAAA AAGCAGGCTCGATGAAGCTTTTGGAGTTGTTCA; PILS4_Rev, GGGGAC CACTTTGTACAAGAAAGCTGGGTC(TCA)TGTCACAAGCCACATGAAGA ATG; PILS5_Fw, GGGGACAAGTTTGTACAAAAAAGCAGGCTCGATGGG ATTCTGGTCGTTGTTGGA; PILS5_Rev, GGGGACCACTTTGTACAAGAAA GCTGGGTC(TCA)GACTAACAAGTGAAGGAAGATGG; PILS6_Fw, GGGGA CAAGTTTGTACAAAAAAGCAGGCTCGATGATTGCTCGGATCCTTGCCG; PILS6_Rev, GGGGACCACTTTGTACAAGAAAGCTGGGTC(TCA)GAAGAG TATGTTAATGTAGAGTAC; PILS7_Fw, GGGGACAAGTTTGTACAAAAAA GCAGGCTCGATGGGTTTCTTAGAGTTGTTGGA; PILS7_Rev, GGGGACCA CTTTGTACAAGAAAGCTGGGTC(TCA)GGAGAGGATGGAGAGGAAGAT GG.

Promoter: PILS2_Fw, GGGGACAACTTTGTATAGAAAAGTTGCGAACTCC ATTGTTAACAGTAATAGC; PILS2_Rev, GGGGACTGCTTTTTTGTACAAA CTTGCCTCGATCTCACTATGTAAAGCTCG; PILS5_Fw, GGGGACAACTT TGTATAGAAAAGTTGCGCAATATACGTGACGTGGTCCACT; PILS5_Rev, GGGGACTGCTTTTTTGTACAAACTTGCCTTTTTATGTGGTTCTTTAGAC.

Destination vectors: *pPILS::GFP/GUS: pKGWFS7*, *p35S::PILS::GFP: pH7FWG2,0*, *p35S::GFP::PILS: pH7WGF2,0*, *p35S::PILS::RFP: pK7RWG2,0*, *p35S::RFP::PILS: pK7WGR2,0* and *p35S::PILS_D: pH7WG2D,1* (ref. 33), and *pPILS::PILS::GFP: pK7m34GW,0* (ref. 34).

Oestradiol-inducible PILS: *pMDC7_B(pUBQ)*[35] (p35S promoter was exchanged by the pUBQ10 promoter).

22. Sauer, M., Paciorek, T., Benkova, E. & Friml, J. Immunocytochemical techniques for whole-mount *in situ* protein localization in plants. *Nature Protocols* **1,** 98–103 (2006).
23. Delbarre, A., Muller, P., Imhoff, V. & Guern, J. Comparison of mechanisms controlling uptake and accumulation of 2,4-dichlorophenoxy acetic acid, naphthalene-1-acetic acid, and indole-3-acetic acid in suspension-cultured tobacco cells. *Planta* **198,** 532–541 (1996).
24. Bailly, A. *et al.* Modulation of P-glycoproteins by auxin transport inhibitors is mediated by interaction with immunophilins. *J. Biol. Chem.* **283,** 21817–21826 (2008).
25. Dobrev, P. I., Havlíček, L., Vágner, M., Malbeck, J. & Kamínek, M. Purification and determination of plant hormones auxin and abscisic acid using solid phase extraction and two-dimensional high performance liquid chromatography. *J. Chromatogr. A* **1075,** 159–166 (2005).
26. Dobrev, P. I. & Kamínek, M. Fast and efficient separation of cytokinins from auxin and abscisic acid and their purification using mixed-mode solid-phase extraction. *J. Chromatogr. A* **950,** 21–29 (2002).
27. Schultz, J., Milpetz, F., Bork, P. & Ponting, C. P. SMART, a simple modular architecture research tool: identification of signaling domains. *Proc. Natl Acad. Sci. USA* **95,** 5857–5864 (1998).
28. Letunic, I., Doerks, T. & Bork, P. SMART 6: recent updates and new developments. *Nucleic Acids Res.* **37,** 229–232 (2009).
29. Tusnády, G. E. & Simon, I. The HMMTOP transmembrane topology prediction server. *Bioinformatics* **17,** 849–850 (2001).
30. Spyropoulos, I. C., Liakopoulos, T. D., Bagos, P. G. & Hamodrakas, S. J. TMRPres2D: high quality visual representation of transmembrane protein models. *Bioinformatics* **20,** 3258–3260 (2004).
31. Proost, S. *et al.* PLAZA: a comparative genomics resource to study gene and genome evolution in plants. *Plant Cell* **21,** 3718–3731 (2009).
32. Pěnčík, A. *et al.* Isolation of novel indole-3-acetic acid conjugates by immunoaffinity extraction. *Talanta* **80,** 651–655 (2009).
33. Karimi, M., De Meyer, B. & Hilson, P. Modular cloning in plant cells. *Trends Plant Sci.* **10,** 103–105 (2005).
34. Karimi, M., Inze, D. & Depicker, A. GATEWAY vectors for *Agrobacterium*-mediated plant transformation. *Trends Plant Sci.* **7,** 193–195 (2002).
35. Curtis, M. D. & Grossniklaus, U. A gateway cloning vector set for high-throughput functional analysis of genes in planta. *Plant Physiol.* **133,** 462–469 (2003).